Optica Applicata, Vol. XL, No. 1, 2010

Numerical optimization of polarizing beam splitter gratings and modal explanation

Bo WANG

School of Physics and Optoelectronic Engineering, Guangdong University of Technology, Guangzhou 510006, China; e-mail: wb_wsx@yahoo.com.cn

We describe high-density deep-etched fused-silica transmission polarizing beam splitter (PBS) gratings and their simple physical explanation. Optimized numerical results of the grating depth and period are given using the rigorous coupled-wave analysis in order to achieve high extinction ratio and efficiency for the usual laser wavelengths 351, 441.6, 532, 632.8, 800, and 1053 nm. The physical mechanism of such a PBS grating can be well explained with the effective indices of the modes for TE/TM polarization, which is a useful extension of the modal method for different structures reported in this paper. Compared with the work of Clausnitzer *et al*., fused-silica gratings can work as PBSs for not only the special duty cycle of 0.51 but also the usual duty cycle of 0.50. These numerical results and simple physical explanation provide a useful guideline for the design of a PBS grating.

Keywords: diffractive optics, rigorous coupled-wave analysis, modal method, polarizing beam splitter.

1. Introduction

Polarizing beam splitters (PBSs) can separate two orthogonally polarized wave beams into different propagation directions, which are widely applied in numerous optical information processing systems [1, 2]. However, conventional PBSs based on birefringent crystals are bulky. And PBSs made of multilayer dielectric coatings are usually expensive and applicable only in a narrow wavelength range. Subwavelength gratings have attracted more and more attention with features of the miniaturization and simple fabrication [3–5]. Recently, a few PBS surface-relief gratings have been reported [6–8]. Based on the excellent optical material of fused silica, Wang *et al*. designed and fabricated both a PBS grating [8] and a two-port beam splitter grating [9] with wideband spectrum around a wavelength of 1550 nm.

Rigorous coupled-wave analysis (RCWA) [10] can be used to calculate the optical properties of a high-density deep-etched grating. However, it is hard to understand the physical mechanism taking place inside the grating region from their numerical treatment. Recently, Clausnitzer *et al*. adopted the modal method [11–13] to

investigate these high-efficiency dielectric rectangular transmission gratings [14] and polarization-dependent diffraction [15]. Such polarization-dependent diffraction can occur for the special duty cycle of 0.51 in reference [15].

In this paper, various optimized numerical results of deep-etched fused-silica transmission PBS gratings are obtained using the RCWA for the widely-used lasers (351, 441.6, 532, 632.8, 800, and 1053 nm). Then, the modal method [11] is applied to give a physical explanation of PBS gratings. Summary of the optimized numerical results provides a useful guideline of design and fabrication of the deep-etched binary phase fused-silica gratings for polarization separation, which is a useful extension of the modal method for explaining physical mechanism of transmission PBS gratings.

2. Numerical optimization

Figure 1 shows a transmission PBS grating, where d is the period, b and g are the ridge and groove widths, respectively, and h is the depth. The duty cycle f is defined as the ratio of the grating ridge width to the period. We consider the PBS as a deep-etched fused-silica grating with refractive index of n_2 for the grating ridges and $n_1 = 1$. A plane wave of wavelength λ illuminates the PBS grating under Littrow mounting of incident angle $\theta_i = \sin^{-1}(\lambda/2d)$. The TE- and TM-polarized waves are diffracted in the 0th and –1st orders, respectively.

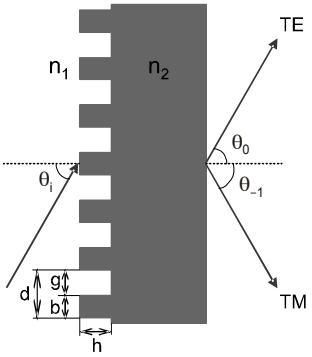

Fig. 1. Schematic of a deep-etched binary phase grating as a polarizing beam splitter.

As shown in Fig. 2, we obtained the extinction ratio of a PBS grating versus period and depth using the RCWA with the refractive index $n_2 = 1.45702$ and duty cycle of 0.50 for the wavelength of 632.8 nm. Figure 2 shows that the extinction ratio can reach the maximum 1.01×10^4 with the period of 482 nm and depth of 1.925 μm. For other widely-used laser wavelengths, we can also optimize the period and depth of PBS gratings using the RCWA in order to achieve the high extinction ratio, which are listed in the Table. However, numerical results given do not help us to know the physical process clearly. It is necessary to explain physical mechanism of PBS gratings. The structures designed in this paper are different from the references [8] and [15]

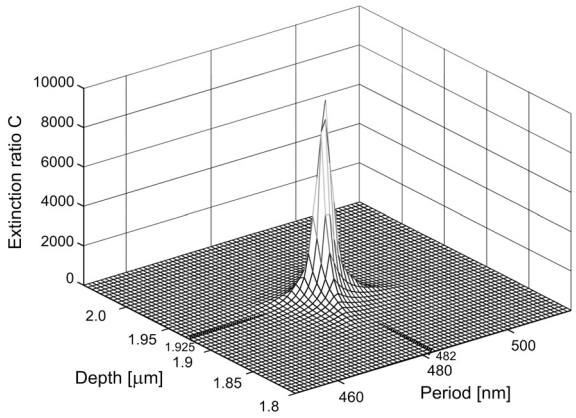

Fig. 2. The extinction ratio of a transmission PBS grating for different profile parameters with duty cycle of 0.50 for the wavelength of 632.8 nm. The highest extinction ratio 1.01×10^4 occurs at the depth of 1.925 μm with the period of 482 nm.

T a b l e. Optimized numerical results of deep-etched fused-silica gratings with the duty cycle f of 0.50 as polarizing beam splitters for the usual laser wavelengths.

	Parameter optimization		TE			TM		
λ [nm]	h [μm]	d [nm]	n_{eff}^0	n_{eff}^1	$\Delta\varphi$	n_{eff}^0	n_{eff}^1	$\Delta\varphi$
351	1.025	264	1.249	0.907	6.275	1.122	0.949	3.174
441.6	1.315	334	1.240	0.905	6.268	1.116	0.947	3.162
532	1.605	404	1.237	0.905	6.293	1.114	0.947	3.166
632.8	1.925	482	1.233	0.905	6.269	1.112	0.946	3.173
800	2.450	609	1.230	0.903	6.292	1.109	0.945	3.156
1053	3.255	805	1.228	0.904	6.293	1.109	0.946	3.166

with the reverse case where the TE- and TM-polarized waves are diffracted in the –1st and 0th orders, respectively. Different effective indices will be excited for the polarization in the 0th order, which cause different tendencies of diffraction efficiencies compared with references [8] and [15].

3. Modal explanation

According to the modal method, the incident wave can excite a discrete set of modes when propagating through the grating region along normal direction [11]. The first two modes with different effective indices will interfere and couple out at the grating--substrate interface [14]. The accumulated phase difference [15] will play a primary role for the efficiency of the 0th and –1st orders during the interference of two modes. On the one hand, the efficiency in the –1st order will be high with the phase difference

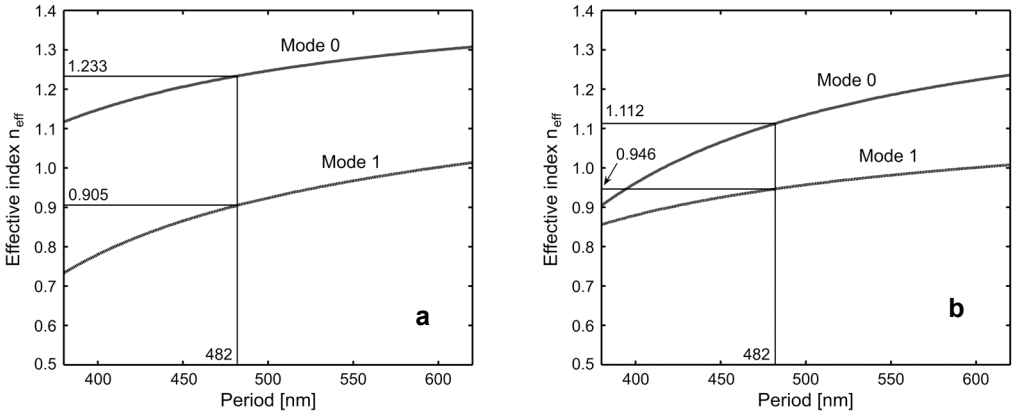

Fig. 3. Effective indices of the first two modes versus the grating period with duty cycle of 0.50 for the wavelength of 632.8 nm: TE polarization (**a**); TM polarization (**b**). The effective indices at period of 482 nm between two modes satisfy the accumulated phase differences $\Delta\varphi = \pi$ and 2π for TM and TE polarizations, respectively (see Fig. 4 and the Table).

of an odd-numbered multiple of π. On the other hand, the efficiency in the 0th order will be high with the phase difference of an even-numbered multiple of π.

Figure 3 shows the effective indices of the first two modes excited by the incident wave versus grating period under Littrow mounting with the incident wavelength of 632.8 nm, duty cycle of 0.50. In Figure 3, effective indices of the excited modes depend on the period with the prescribed duty cycle under Littrow mounting. Furthermore, the two modes in the grating region excited by the incident wave have different effective indices for TE- and TM-polarized waves, respectively. However, in references [8] and [15], the incident wave will excite two modes with the same effective index for TM polarization. For different effective indices, higher aspect ratios of grating depth to ridge width will be needed to modulate the efficiency to obtain PBS gratings in this paper.

Figure 4 shows the phase difference of the first two modes as a function of the period for the depth of 1.925 μm, duty cycle of 0.50, and the wavelength of 632.8 nm. As shown in Figure 4, the phase difference is 2π for TE-polarized wave and π for TM-polarized wave with period of 482 nm, prescribed depth of 1.925 μm. The Table summarized the optimized numerical results of PBS gratings for the usual laser wavelengths using the RCWA. The $\Delta\varphi$ column for TE polarization in the Table is near to $2\pi \approx 6.283$, while $\Delta\varphi$ column for TM polarization in the Table is near to $\pi \approx 3.142$. The optimized profiles of PBS gratings by numerical calculation based on the RCWA coincide well with predictions of the modal method.

However, it is necessary to illustrate that such polarization-dependent diffraction can occur for not only the special duty cycle of 0.51 in reference [15] but also the usual duty cycle of 0.50 in reference [8]. For the special duty cycle of 0.51 in Fig. 7**b** of reference [15], diffraction efficiencies of TM polarization are always less than 0.10% and small deviation from the given duty cycle of 0.51 such as 0.50 can

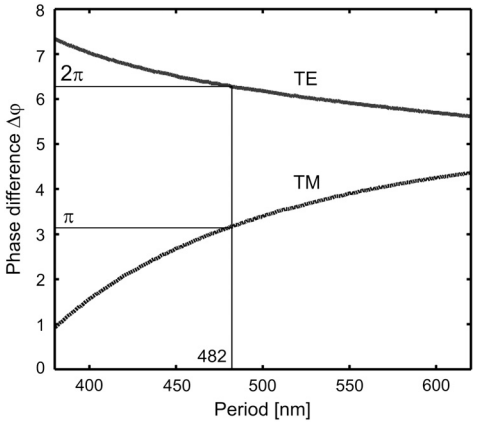

Fig. 4. Phase differences of the first two modes versus the period for the depth of 1.925 μm, duty cycle of 0.50, and the wavelength of 632.8 nm.

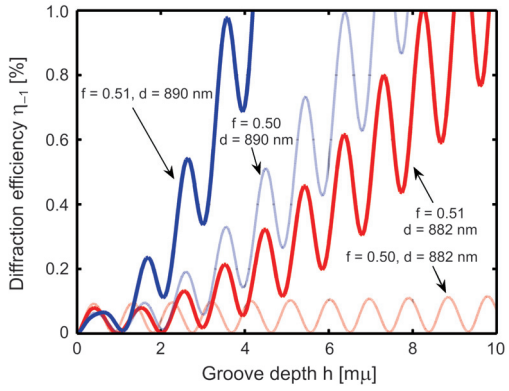

Fig. 5. Diffraction efficiency of TM polarization in the –1st order as a function of the grating depth with the different duty cycle (0.50, 0.51) and period (882, 890 nm) for the wavelength of 1550 nm.

make the efficiency increase with the depth. Figure 5 shows the efficiency of TM polarization as a function of the grating depth with the different duty cycle (0.50, 0.51) and period (882, 890 nm) for the wavelength of 1550 nm. In Figure 5, for a duty cycle of 0.50 with period of 882 nm, the efficiency oscillates up to 0.12% with the depth, while for a duty cycle of 0.51, the efficiency increases with the depth rapidly. Compared with the numerical results of the period of 882 nm, the efficiency increases more rapidly with the depth of the period of 890 nm in reference [8] theoretically. However, in fabrication, such a small deviation of the optimized period does not affect the efficiency much for the optimized depth of near 1.99 μm. Generally speaking, one can see that the polarization-dependent diffraction described in reference [15] can also occur for the duty cycle of 0.50 instead of 0.51. The numerical results from the RCWA in reference [8] imply a different structure to realize the same polarization-dependent diffraction with reference [15].

4. Conclusions

In conclusion, in this paper, numerical simulations of deep-etched fused-silica transmission gratings for PBSs are presented for the usual laser wavelengths, where

TE- and TM-polarized waves are diffracted in the 0th and –1st orders, respectively. In order to obtain high extinction ratio and efficiency, the grating depth and period are optimized using the RCWA. Results obtained using the RCWA correspond well with predictions of the modal method.

It should be noted that although the physical mechanism comes from the same modal theory [11, 14, 15], there are still some differences in the presented design and explanation from the reported papers [8, 15]. First, diffraction processes in the 0th order are different. In this paper, the TE- and TM-polarized waves are diffracted in the 0th and –1st orders, respectively, while references [8] and [15] are based on the reverse case. The design described in this paper will excite two modes with the different effective index for TE polarization. After propagating through the grating region, phase differences of 2π will be accumulated so that the TE-polarized wave is diffracted in the 0th order. However, two modes with the same effective index are excited in references [8] and [15] for TM polarization, and no phase difference will be accumulated so that the TM-polarized wave is diffracted in the 0th order. Second, in this paper, the efficiency changes with grating depth cosinoidally for both TE and TM polarization. Much higher aspect ratios of grating depth to ridge width are needed to obtain PBS gratings. Whereas in references [8] and [15], the TM-polarized wave is mainly diffracted in the 0th order regardless of the grating depth due to the same effective index of the excited modes. Third, this paper studied the influence of the aspect ratio with the usual duty cycle of 0.50, while reference [15] investigates polarization-dependent diffraction of high-density gratings with the special duty cycle of 0.51. In addition, the duty cycle of 0.50 reported in reference [8], as shown in Fig. 5, is also different from 0.51 in reference [15]. Therefore, numerical results and explanation described in this paper for the usual laser wavelengths should provide useful data for fabrication of PBS gratings for practical applications.

Acknowledgement – This work is supported by the Natural Science Foundation of Guangdong Province, China (9451009001002756).

References

[1] ZHOU L., LIU W., *Broadband polarizing beam splitter with an embedded metal-wire nanograting*, Optics Letters **30**(12), 2005, pp. 1434–1436.

[2] LAJUNEN H., TURUNEN J., TERVO J., *Design of polarization gratings for broadband illumination*, Optics Express **13**(8), 2005, pp. 3055–3067.

[3] CLAUSNITZER T., LIMPERT J., ZÖLLNER K., ZELLMER H., FUCHS H.-J., KLEY E.-B., TÜNNERMANN A., JUPÉ M., RISTAU D., *Highly-efficient transmission gratings in fused silica for chirped pulse amplification systems*, Applied Optics **42**(34), 2003, pp. 6934–6938.

[4] ZHANG Y., ZHOU C., *High-efficiency reflective diffraction gratings in fused silica as (de)multiplexers at 1.55 μm for dense wavelength division multiplexing application*, Journal of the Optical Society of America A **22**(2), 2005, pp. 331–334.

[5] WANG S., ZHOU C., ZHANG Y., RU H., *Deep-etched high-density fused-silica transmission gratings with high efficiency at a wavelength of 1550 nm*, Applied Optics **45**(12), 2006, pp. 2567–2571.

[6] LALANNE P., HAZART J., CHAVEL P., CAMBRIL E., LAUNOIS H., *A transmission polarizing beam splitter grating*, Journal of Optics A: Pure and Applied Optics **1**(2), 1999, pp. 215–219.

[7] DELBEKE D., BAETS R., MUYS P., *Polarization-selective beam splitter based on a highly efficient simple binary diffraction grating*, Applied Optics **43**(33), 2004, pp. 6157–6165.

[8] WANG B., ZHOU C., WANG S., FENG J., *Polarizing beam splitter of a deep-etched fused-silica grating*, Optics Letters **32**(10), 2007, pp. 1299–1301.

[9] WANG B., ZHOU C., FENG J., RU H., ZHENG J., *Wideband two-port beam splitter of a binary fused-silica phase grating*, Applied Optics **47**(22), 2008, pp. 4004–4008.

[10] MOHARAM M.G., GRANN E.B., POMMET D.A., GAYLORD T.K., *Formulation for stable and efficient implementation of the rigorous coupled-wave analysis of binary gratings*, Journal of the Optical Society of America A **12**(5), 1995, pp. 1068–1076.

[11] BOTTEN I.C., CRAIG M.S., MCPHEDRAN R.C., ADAMS J.L., ANDREWARTHA J.R., *The dielectric lamellar diffraction grating*, Optica Acta **28**(3), 1981, pp. 413–428.

[12] TISHCHENKO A.V., *Phenomenological representation of deep and high contrast lamellar gratings by means of the modal method*, Optical and Quantum Electronics **37**(1–3), 2005, pp. 309–330.

[13] SHENG P., STEPLEMAN R.S., SANDA P.N., *Exact eigenfunctions for square-wave gratings: Application to diffraction and surface-plasmon calculations*, Physical Review B **26**(6), 1982, pp. 2907–2916.

[14] CLAUSNITZER T., KÄMPFE T., KLEY E.-B., TÜNNERMANN A., PESCHEL U., TISHCHENKO A.V., PARRIAUX O., *An intelligible explanation of highly-efficient diffraction in deep dielectric rectangular transmission gratings*, Optics Express **13**(26), 2005, pp. 10448–10456.

[15] CLAUSNITZER T., KÄMPFE T., KLEY E.-B., TÜNNERMANN A., TISHCHENKO A.V., PARRIAUX O., *Investigation of the polarization-dependent diffraction of deep dielectric rectangular transmission gratings illuminated in Littrow mounting*, Applied Optics **46**(6), 2007, pp. 819–826.

Received July 8, 2009
in revised form August 3, 2009